# Estimating the Absorbed Dose to Critical Organs During Dual X-ray Absorptiometry

M Mokhtari-Dizaji, PhD[1]
A A Sharafi, PhD[2]
B Larijani, MD[3]
N Mokhlesian, MSc[4]
H Hasanzadeh, MS[1]

**Objective:** The purpose of this study is to estimate a patient's organ dose (effective dose) during performance of dual X-ray absorptiometry by using the correlations derived from the surface dose and the depth doses in an anthropomorphic phantom.

**Materials and Methods:** An anthropomorphic phantom was designed and TLDs (Thermoluminescent Dosimeters) were placed at the surface and these were also inserted at different depths of the thyroid and uterus of the anthropomorphic phantom. The absorbed doses were measured on the phantom for the spine and femur scan modes. The correlation coefficients and regression functions between the absorbed surface dose and the depth dose were determined. The derived correlation was then applied for 40 women patients to estimate the depth doses to the thyroid and uterus.

**Results:** There was a correlation between the surface dose and depth dose of the thyroid and uterus in both scan modes. For the women's dosimetry, the average surface doses of the thyroid and uterus were 1.88 $\mu$Gy and 1.81 $\mu$Gy, respectively. Also, the scan center dose in the women was 5.70 $\mu$Gy. There was correlation between the thyroid and uterus surface doses, and the scan center dose.

**Conclusion:** We concluded that the effective dose to the patient's critical organs during dual X-ray absorptiometry can be estimated by the correlation derived from phantom dosimetry.

**Index terms:**
Dual X-ray absorptiometry
TLD dosimetry
Phantom
Absorbed dose
Critical organs

DOI:10.3348/kjr.2008.9.2.102

***Korean J Radiol 2008;9:102-110***
Received March 19, 2007; accepted after revision July 26, 2007.

[1]Medical Physics Department, Tarbiat Modares University, Tehran, Iran; [2]Medical Physics Department, Iran University of Medical Sciences, Tehran, Iran; [3]Metabolism and Endocrine Research Center, Tehran Medical Sciences University, Tehran, Iran; [4]Medical Radiation Department, Azad University, Tehran, Iran

**Address reprint requests to:**
M. Mokhtari-Dizaji, Associate Professor, Department of Medical Physics, Tarbiat Modares University, Tehran, Iran.
Tel. 98-21-82883893
Fax. 98-21-82886544
e-mail: mokhtarm@modares.ac.ir

Osteoporosis is the most common cause of bone fractures in women, and especially during their menopausal period (1, 2). Bone densitometry is an effective tool for assessing the risk of bone fracture. Today, it is also possible to control bone density during the healing period. Dual-energy X-ray absorptiometry (DXA) is the most applicable method to assess bone density, and this also allows for the determination of the bone mineral density (BMD) and bone mineral content (BMC). Radiation protection standards have been developed with the advent of bone densitometry, which utilizes ionizing radiation. Previous studies have shown that for performing bone densitometry with the DXA method, the radiation dosage to critical organs is due to scattered radiation; the surface doses from different DXA systems (pencil, fan and cone beams) have also been measured and compared. A recent study measured the values of the surface doses originating from a cone beam of the new DXA systems (3).

Due to radiation protection and the ALARA (As Low As Reasonably Achievable) standards, the assessment of radiation exposure requires performing radiation dosimetry (4). Manufacturers usually place emphasis on the surface dose, but this quantity is

not enough to estimate the patients' risk. It is also necessary to determine the absorbed and effective doses.

The majority of studies in the field of dosimetry that have used DXA systems have compared surface doses from pencil and fan beams (5, 6). The patients' effective dose was calculated in those studies on the systems that utilize a fan beam, and the effective dose was proven to be smaller than that using other conventional radiography techniques (7, 4). A bone equivalent humanoid spine phantom was used in several previous studies to evaluate the surface doses from systems with a fan beam (5, 6, 8-12). The surface doses on two phantoms that were five and 10 years old, respectively, from a system with a pencil beam, were measured using TLDs (Thermoluminescent Dosimeters). In that study, the TLDs showed a small value (~0) for the absorbed dose. The necessity of utilizing dosimetry for these systems was nonetheless highlighted (13). In another study, it was shown that the effective dose from a fan beam was about two times greater than that from a pencil beam. However, those values are still smaller than the effective dose of the conventional radiography methods (14, 15). In another study that aimed to estimate the embryo radiation doses and the risks associated with spinal and hip DXA, it was shown that the use of an apron resulted in a very small change in the absorbed dose to the embryo (16).

Today's DXA systems have evolved from using pencil and fan beams to using cone beam densitometers, which allows for an examination to occur without any scanning and with a short acquisition time. It was shown that the patient and staff doses from DXA systems are low (3).

Although new methods for bone densitometry have been developed, there have been no studies to estimate the absorbed dose to critical organs on the basis of the surface dose using DXA systems. Therefore, in this study, a tissue equivalent anthropomorphic phantom was irradiated with the femur and spine protocols. Using TLDs that were placed at the surface and at different depths of the thyroid and uterus, the absorbed dose of a Lunar DPX-MD densitometer with a pencil beam was measured. Forty women also underwent bone densitometry with a Lunar DPX-MD system, which utilizes a pencil beam, in the posteroanterior (PA) spine and femur scan modes. The surface doses of the thyroid, uterus and center of the scan point were measured using TLDs. The percentage of surface dose per unit dose to the center of the scan for the thyroid and uterus was then calculated. Based on the correlation coefficients and linear regression functions between the phantom surface dose and the dose at different depths, the thyroid and uterus depth doses were then estimated. The correlation between the scan center dose and surface dose to critical organs was then calculated. Finally, the effective doses to the thyroid and uterus were compared with the background radiation dose.

## MATERIALS AND METHODS

### *DPX-MD Densitometer*

The Lunar DPX-MD is one of the most widely used DXA machines. It uses a pencil X-ray beam that's detected after passing through the patient. Both the X-ray source and detector traverse the scanning area with a rectilinear motion. The DPX-MD (Lunar Corp., DPX series, Lunar MD 7164, WI, with a scan speed of 1 mm/s and a resolution of 0.5 $\times$0.5 mm) has a highly stable potential X-ray generator with a k-edge filter. The two X-ray energies required to differentiate between soft tissue and bone are produced using this filter. The X-ray tube is operated at 76 kVp and it has a maximum current of 5 mA. The effective energies of the beam are 38 and 70 keV. The operating current of the system is 0.75 mA. Its filtration is 35 mm-Al and the maximum field size is $10 \times 10$ mm$^2$. The distance from the focal spot of the X-ray tube to the patient is 33.0–33.5 cm and the distance from the focal spot to the detector is 58.2 cm. The system is capable of evaluating bone density in the spine and femur, and it is also used for total body protocols. In spine scan mode, the scan area is $20 \times 18$ cm$^2$ with a maximum line scan of 167 lines and a scan width of 18 cm. The scan width is 15 cm in the femur scan mode. The scanned-area BMD and BMC data can be displayed with the DPX-MD software (version 4).

Various scanning modes (slow, medium and fast) can be used depending on the weight/thickness of the abdomen of the patient and the required resolution. In this study, the slow mode was assessed, which has a longer exposure time.

### *TLD Measurement Technique*

Radiation dosimetry measurements were made using cubic calcium flouride TLDs ($3 \times 3 \times 1$ mm$^3$). The TLDs (TLD-400; Harshaw/Bicron, Solon, OH) were initially sorted into groups of equal sensitivity by a calibration procedure. The first step in this procedure was to obtain the ECCs (Element Correction Coefficients), which were applied in order to increase the reproducibility because of the individual differences between the TLD responses. On average, TLD badges have variations in the range of 10-15% which, after applying ECCs, was reduced to about 1-2%. We exposed 18 TLDs (76 kVp, 100 cm FFD, 100 mA, 0.01 S) and obtained their responses ($x_i$), and we calculated the mean of their responses ($x_{AV}$) in nC (nano Coulombs). The ECC for each TLD was obtained from the equation:

$$ECC = \frac{x_{AV}}{x_i}$$

To obtain the calibration equation, we used 20 TLDs: six groups of three TLDs and two TLDs for background radiation measurements. These six groups were exposed to 13.94, 31.40, 44.23, 70.79, 92.80 and 133 $\mu$Gy. The readout procedure was done using a TLD reader (TLD reader, Harshaw 3500). To obtain each of these doses, a multimeter (Unfors 401, Sweden) with accuracy of $\pm$ 1 $\mu$Gy was placed in the radiation field. To increase the accuracy and reproducibility, each exposure was repeated three times. The TLDs were then annealed for one hour at 500°C (Atash 1200 Exiton Corp., Iran). According to the results, the dose ($\mu$Gy) versus reading (nC) was plotted, and a calibration curve was obtained (Fig. 1).

To increase the measurement and calculation accuracy, we created four groups that each consisted of three TLDs, and the three TLDS in each group were exposed to 21.23, 56.05, 80.23 and 105.7 $\mu$Gy, respectively, and these dose values were measured by a multimeter. After reading and applying the ECCs and obtaining dose values from the calibration equation, mean values for each group were calculated as 23.41, 57.08, 78.36 and 103.98 $\mu$Gy. Calculated versus real values were plotted, and a correction factor was obtained (Fig. 2).

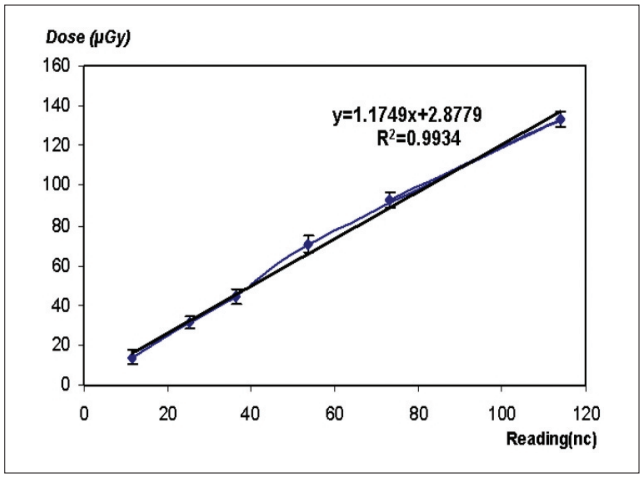


**Fig. 1.** Calibration curve of TLDs.

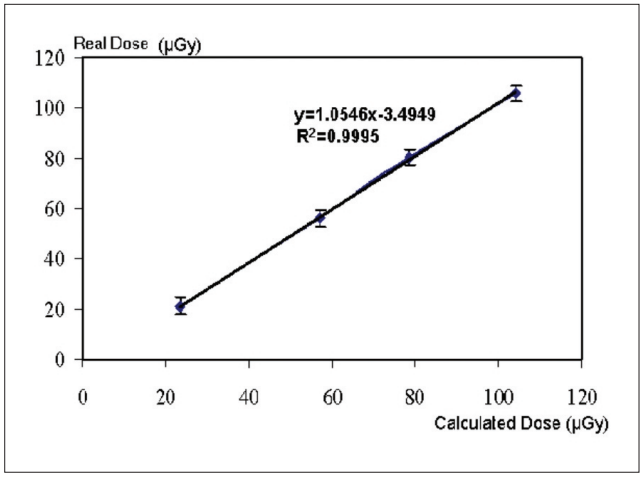


**Fig. 2.** Correction factor curve for TLDs.

### *Anthropomorphic Phantom*

To estimate the absorbed dose to critical organs at different depths versus the surface dose, we used an anthropomorphic phantom that consists of three parts: the head and neck, the abdomen and the pelvic areas. This phantom was designed and constructed at the Iran University of Medical Sciences. Natural bone was used in the construction of this phantom. Paraffin wax with NaCl (impurity) was used as a substitute for soft tissues. The effective atomic number and electron density of the soft tissue material were 6.57 and $3.36 \times 10^{23}$ $g^{-1}$, respectively. For the lungs, two spongy woods were prepared with dimensions similar to the lungs, but with lower density than the soft tissue. Several probes made of phantom material that had TLDs located at different depths (with 1 cm intervals) were constructed for the dosimetry of the critical organs (Fig. 3).

### *Phantom Measurement*

Phantom dosimetry was done using two different protocols for the spine and femur, respectively. The scanning conditions were complementary to the normal scan modes. First, a PA spinal scan was done in slow mode with 450 mAs; the absorbed dose to thyroid, uterus and scan center (the lumbar region) were then measured at the organ surface and the different depths (Fig. 4). To reduce error, each badge consisted of three TLDs. To measure the thyroid dose in this scan, badges with three TLDs were prepared and placed at the right and left lobes of the

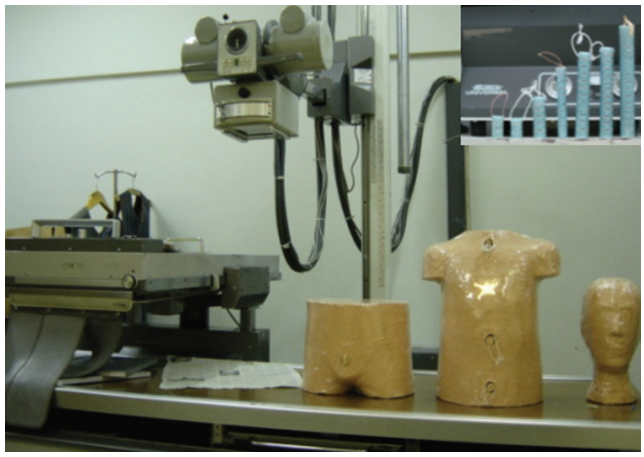

**Fig. 3.** Front view of anthropomorphic phantom with depth probes.

thyroid at the surface and at different depths. One badge was placed at the scan center. Two additional TLDs were used to measure the background radiation outside the room. After applying the correction and calibration coefficients for each TLD, the dose to each region was then calculated in $\mu$Gy. We then applied X-ray quality factor and thyroid weighting factor to obtain the effective dose equivalent in $\mu$Sv. To estimate the surface and depth doses to the phantom in the uterus region in PA spine scan mode, TLD badges were placed at the surface and at 12.5 cm, 17.5 cm and 22 cm depth within the phantom. To reduce error, each scan was repeated four times. Because the uterus and ovaries are in the same region, radiation quality factor and tissue weighting factor were applied and their contribution to the dose equivalent was assessed.

In the femur scan protocol, that is, in the slow mode with 270 mAs, only the uterus dose was assessed due to the very low thyroid exposure, which was found to be in the range of the background radiation (a large distance from the thyroid to the femur center of the scan). To measure dose values, badges with three TLDs were placed at ten different depths in the uterus, and this included the surface, 9.5, 10.5, 11.5, 12.5 (center of uterus), 14.5, 15.5, 16.5, 17.5 (above uterus) and 22 cm from the source. To reduce error, the femur scan was repeated five times. After acquisition of the dose values, correlations between the depth and the surface dose of the critical organs were assessed. In cases where the correlation coefficients were significant, linear regression analysis was done to estimate the depth dose of critical organs versus their surface dose.

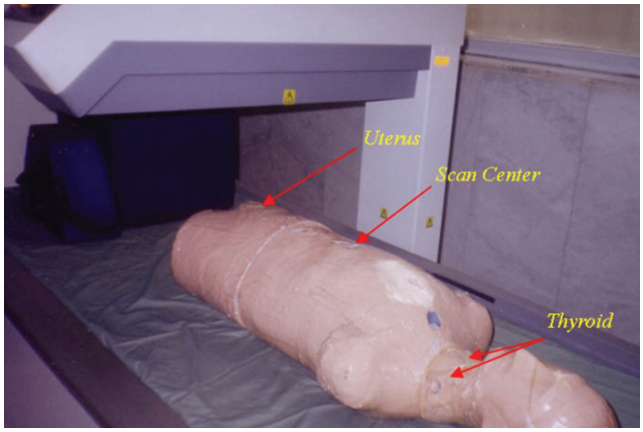


**Fig. 4.** Anthropomorphic phantom in measurement position.

### *Patient Measurement*

The patients included in this study consisted of 40 women who were referred to the Iran Metabolism and Endocrine Research Center for bone densitometry. This study was performed from Jan 2005 to Feb 2006 and it was approved by the Ethics Committees of the Iran Metabolism and Endocrine Research Center (Iran). First, a list of each patient's characteristics including age, height, weight, body thickness and body mass index (BMI) was obtained along with written consent before each experiment (Table 1). The system current for each patient was proportional to the patient's BMI in each of the PA spine and femur protocols (397 $\pm$57 mAs). The number of femur scan lines for each patient was proportional to their weight and height.

In the PA spine scan, the area between the first and forth vertebrae (L1-L4) was scanned. To assure the accuracy of the patient position, a scan was also done from T12-L5. In the femur scan, one of the patient's legs was rotated from ankle eversion. The patient measurements badges were placed at the following locations: two badges at the scan center (between L1-L4), two at the location of the thyroid lobes, two at the location of the uterus and two at the center of the femur scan position. All of these badges were placed at the surface and on the posterior side of the patient to measure the surface dose. Two badges were used to monitor the background radiation. For each patient, a scan protocol that included the PA, spine and femur modes was utilized. The patient entrance dose at the location of the critical organs and the dose at the scan center were measured together with the background radiation using TLDs. After acquiring the dose values,

**Table 1. Mean and Standard Deviation of Patients' Characteristics**

| Age (yr) | Height (cm) | Weight (kg) | Thickness (cm) | BMI ($kg.m^{-3}$) |
|---|---|---|---|---|
| 55 $\pm$12 | 157 $\pm$7 | 67 $\pm$10 | 20 $\pm$2 | 26.3 $\pm$4.4 |

Note.—BMI = body mass index

**Table 2. Mean and Standard Deviation of Surface Dose ($D_S$) and Depth Dose of Thyroid (Dd; depth length, cm), Scan Center and Background Doses ($\mu$Gy)**

| Right Lobe (n* = 24) | | Left Lobe (n = 24) | | Scan Center (n = 12) | Background (n = 8) |
|---|---|---|---|---|---|
| $D_d$ (7 cm) | $D_S$ (0) | $D_d$ (7 cm) | $D_S$ (0) | | |
| 1.16 $\pm$ 0.15 | 1.21 $\pm$ 0.20 | 1.23 $\pm$ 0.27 | 1.37 $\pm$ 0.27 | 6.15 $\pm$ 1.22 | 1.01 $\pm$ 0.25 |

Note.—* Number of measurements

correlations between the dose at the scan center and the surface dose at critical organs were assessed. If the correlation coefficient was significant, then linear regression analysis was done to estimate the dose to critical organs versus the dose at the scan center. These organs are not in the scan direction; therefore, their absorbed dose is due to scattered radiation from other tissues. The percentage surface dose (D) to an organ was calculated based on the organ surface dose ($D_0$) and the total radiation dose of each scan ($D_t$) and the scan center dose with using the following equation:

$$D = \frac{D_0}{D_t} \times 100$$

The depth dose to the thyroid and uterus was estimated from the values of the previous phantom studies. The contribution of these organs to the effective dose ($H_E$ [$\mu$Sv]) was summed from the following equation:

$$H_E = \sum_{T=1}^{n} H_T \times W_T$$

where $H_T$ is the dose equivalent and it is derived from the product of the absorbed dose ($\mu$Gy) and the radiation quality factor (for X-rays, the quality factor is unity). $W_T$ is a tissue weighting factor, which differs for different tissues.

All of the statistical analyses were calculated with SPSS (SPSS/PC Inc; Chicago, version 11.5). *P*-values less than 0.01 were chosen as the level of statistical significance.

## RESULTS

### *Phantom*

The results of the thyroid dose in the PA spine scan mode are shown in Table 2. The TLD badges were placed at the right and left lobes (at the surface and depth) and at the scan center and the results were analyzed after each of four runs.

In this scan, the average thyroid dose was 1.28 ±0.25 $\mu$Gy for the left lobe and 1.18 ±0.17 $\mu$Gy for the right lobe. By applying a thyroid weighting factor (0.05), the effective dose for the left and right lobes was found to be 0.06 ±0.01 $\mu$Sv and 0.06 ±0.02 $\mu$Sv, respectively. Correlation analysis was performed to obtain a relationship between the depth and surface dose in the thyroid. When the correlation coefficient was significant, a linear regression function was obtained. The results from the linear regression analysis are shown in Table 3.

However, in this study, there was no significant correlation between the thyroid dose and the dose at the scan center.

To assess the uterus dose in the PA spine scan mode, the absorbed dose at four depths in the uterus (four times for each protocol and using three TLDs in each badge) was measured. The results from assessing the uterus depth dose at zero distance (at the surface near the source), 12.5 cm (center of uterus), 17.5 cm (above the uterus) and 22 cm (the surface at the anterior position of phantom) from the source, the background dose and the dose at the scan center are shown in Table 4.

In this scan, the uterus average dose in the PA spine scan mode was 1.21 ±0.33 $\mu$Gy. According to the similar position of the uterus and ovaries and taking into account the uterus and ovaries weighting factors of 0.05 and 0.20, respectively, their contribution to the effective dose was 0.06 ±0.02 $\mu$Sv for the uterus and 0.24 ±0.07 $\mu$Sv for the ovaries.

Pearson correlation and linear regression analysis were applied to obtain the correlation between the depth and

**Table 3. Linear Regression Functions and Correlation Coefficients for Independent Variable of Surface Dose ($D_S$) and Dependent Variable of Depth Dose ($D_d$) for Thyroid**

| Organ | Linear Regression Functions | Correlation Coefficient | *p* value |
|---|---|---|---|
| Thyroid left lobe | $D_d = 0.57 \times D_S + 0.61$ | 0.69 | 0.014 |
| Thyroid right lobe | $D_d = 0.47 \times D_S + 0.62$ | 0.65 | 0.024 |

**Table 5. Linear Regression Functions and Correlation Coefficients for Independent Variable of Surface Dose ($D_S$) and Dependent Variable of Depth Dose ($D_d$; depth length, cm) for Uterus at Different Depths**

| Linear Regression Function | Correlation Coefficient | Significant Level |
|---|---|---|
| $D_{12.5} = 0.94 \times D_S + 0.14$ | 0.60 | 0.039 |
| $D_{17.5} = 1.52 \times D_S + 0.44$ | 0.77 | 0.003 |
| $D_{22.0} = 0.76 \times D_S + 0.30$ | 0.86 | 0.000 |

**Table 4. Mean and Standard Deviation of Surface Dose ($D_S$) and Uterus Depth Dose (Dd; depth length, cm) at Zero Distance (at Surface Near Source), 12.5 cm (Center of Uterus), 17.5 cm (above Uterus), 22 cm (Surface at Anterior Position of Phantom), Dose at Scan Center and Background Dose ($\mu$Gy): PA Spinal Scan Mode**

| $D_S$ (n* = 12) | $D_d$ (12.5) (n = 12) | $D_d$ (17.5) (n = 12) | $D_d$ (22.0) (n = 12) | Scan Center (n = 12) | Background (n = 8) |
|---|---|---|---|---|---|
| 1.13 ± 0.21 | 1.21 ± 0.33 | 1.29 ± 0.42 | 1.16 ± 0.19 | 6.58 ± 1.19 | 1.04 ± 0.34 |

Note.—* Number of measurements

surface doses in the uterus. Table 5 shows the regression functions between the depth and surface dose in the uterus with their significance levels and correlation coefficients.

There was no significant correlation between the uterus surface dose and the depth dose and the dose at the scan center ($p$-value < 0.05).

In the femur scan protocol, uterus dosimetry (with 270 mAs exposure) was done at 10 different depths; this included the surface dose (near the source), 9.5, 10.5, 11.5, 12.5 (center of the uterus), 14.5, 15.5, 16.5, 17.5 (above the uterus) and 22.0 cm from the surface. To reduce the error, the femur scan protocol was repeated five times. Table 6 shows the results from the analysis of doses at different depths. In this protocol, the dose at the scan center and the background dose were 7.38 ±2.27 μGy and 2.23 ±1.25 μGy, respectively. In this protocol, the uterus absorbed dose was 2.52 ±1.12 μGy. After applying the uterus and ovary weighting factors, their contributions to the effective dose equivalent were found to be 0.13 ±0.06 μSv and 0.50 ±0.22 μSv, respectively.

To evaluate a linear regression between the absorbed uterus dose at the surface and at different depths, correlation regression analysis with linear regression was performed with the results being given in Table 7.

*Patient*

The surface dose of the thyroid, uterus, center of the scan and background in the PA spine and femur scan modes for 40 women (patients) with using 120 TLDs are shown in Table 8.

Pearson correlation analysis between the dose at the scan center and the thyroid and uterus surface dose showed that there is a significant correlation between the two; therefore, linear regression analysis was applied. The results of the regression analysis are listed in Table 9.

Therefore, we can measure the dose at the scan center and assess the dose to critical organs. Also, there was a significant correlation (a correlation coefficient of 0.94 and a $p$-value < 0.001) between the thyroid and uterus surface doses in both the PA spinal and femur scan modes. The average distances from the thyroid and uterus to the edge of the PA spine scan were 37.18 and 26.39 cm, respectively. The distances from the thyroid and uterus in the femur scan were 59.47 and 6.27 cm, respectively. The percentage the surface dose of the thyroid and uterus organs with respect to the center of scan dose is shown in Table 10.

Finally, we used phantom linear regression functions to estimate the depth dose according to the surface dose in the patients. The results are listed in Table 11. After

**Table 6. Mean and Standard Deviation of Surface Dose ($D_S$: Near Source) and Depth Dose ($D_d$; depth length, cm) at 9.5, 10.5, 11.5, 12.5 (Center of Uterus), 14.5, 15.5, 16.5, 17.5 (above Uterus) and 22.0 cm from Surface (μGy) (n = 15)**

| $D_d$ (0) | $D_d$ (9.5) | $D_d$ (10.5) | $D_d$ (11.5) | $D_d$ (12.5) | $D_d$ (14.5) | $D_d$ (15.5) | $D_d$ (16.5) | $D_d$ (17.5) | $D_d$ (22.0) |
|---|---|---|---|---|---|---|---|---|---|
| 2.27 ±0.88 | 2.40 ±1.42 | 3.49 ±0.73 | 2.89 ±0.35 | 2.74 ±0.13 | 2.45 ±0.89 | 4.52 ±1.31 | 2.87 ±0.08 | 3.22 ±0.41 | 2.93 ±1.56 |

**Table 7. Linear Regression Functions and Correlation Coefficients for Independent Variable of Surface Dose ($D_S$) and Dependent Variable of Depth Dose ($D_d$) for Uterus at Different Depths**

| Linear Regression Function | Correlation Coefficient | Significant Level |
|---|---|---|
| $D_{22.0} = 1.54 \times D_S - 0.56$ | 0.87 | 0.000 |
| $D_{14.5} = 0.90 \times D_S + 0.53$ | 0.93 | 0.006 |
| $D_{9.5} = 1.48 \times D_S + 0.74$ | 0.97 | 0.002 |

**Table 8. Mean and Standard Deviation of Surface Dose ($D_S$) of Thyroid, Uterus, Center of Scan and Background in PA Spine and Femur Scan Modes for 40 Women (Patients) with Using 120 TLDs (μGy)**

| $D_S$ Thyroid | $D_S$ Uterus | Center of Scan | Background |
|---|---|---|---|
| 1.88 ± 1.36 | 1.81 ± 1.03 | 5.70 ± 2.38 | 1.45 ± 0.98 |

**Table 9. Linear Regression Functions and Correlation Coefficients for Independent Variable of Surface Dose ($D_S$) and Dependent Variable of Center of Scan Dose ($D_C$)**

| Linear Regression Function | Correlation Coefficient | Significant Level |
|---|---|---|
| $D_S$ (Thyroid) = $0.40 \times D_C - 0.38$ | 0.55 | 0.000 |
| $D_S$ (Uterus) = $0.27 \times D_C + 0.38$ | 0.69 | 0.000 |

**Table 10. Mean and Standard Deviation of Percentage of Surface Dose of Thyroid and Uterus Organs with Respect to Center of Scan Dose ($D_C$)**

| Dc(μGy) | Percent of Relative Absorbed Dose (Thyroid) | Percent of Relative Absorbed Dose (Uterus) |
|---|---|---|
| 5.70 ± 2.38 | 33 ± 13 | 35 ± 13 |

**Table 11. Estimation of Depth Dose of Thyroid and Uterus Organs (Dd; depth length, cm) based on Their Surface Dose (μGy) with Using Extracted Linear Regression Functions of Phantom**

| Uterus Femur Scan Mode | | | Uterus PA Spine Scan Mode | | | Thyroid PA Spine Scan Mode | |
|---|---|---|---|---|---|---|---|
| $D_d$ (9.5) | $D_d$ (14.5) | $D_d$ (22.0) | $D_d$ (12.5) | $D_d$ (17.5) | $D_d$ (22.0) | Left lobe | Right lobe |
| 3.42 ±1.52 | 2.23 ±1.23 | 2.23 ±1.59 | 1.85 ±0.97 | 2.30 ±1.57 | 1.67 ±0.78 | 1.51 ±0.64 | 1.69 ±0.78 |

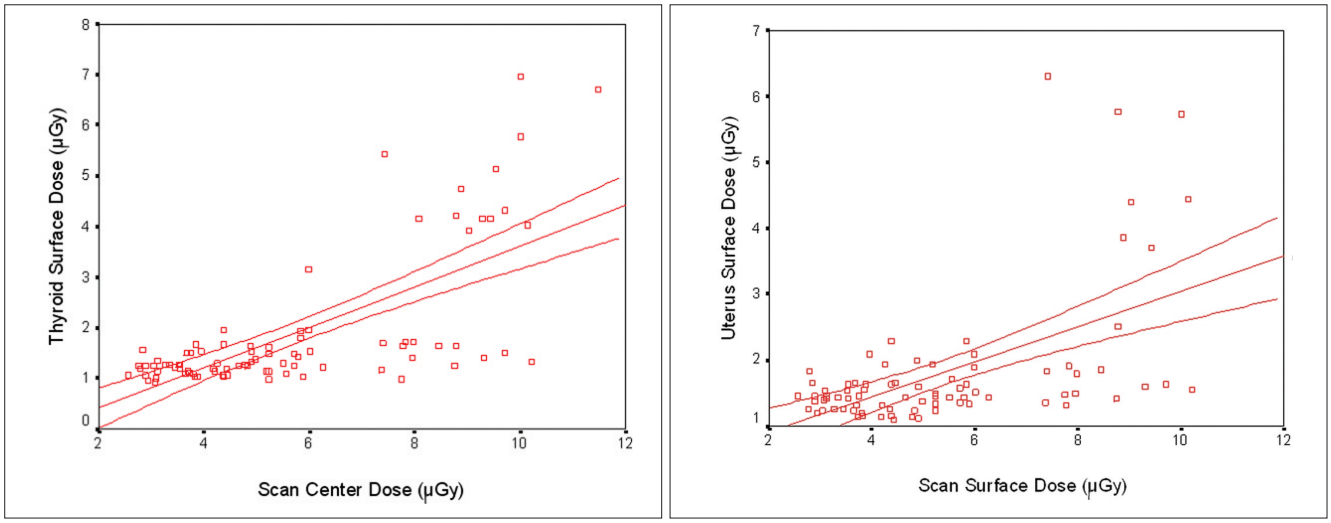


A B

**Fig. 5.** Scatter plot between centers of scan dose with thyroid surface dose (**A**) and uterus surface dose (μGy) (**B**) with 95% confidence interval.

applying X-ray quality factor and thyroid and uterus weighting factors (0.05), the mean thyroid contribution to the effective dose was found to be 0.08 μSv. The uterus contribution was 0.13 μSv in the PA spinal scan mode and 0.14 μSv in the femur scan mode.

## DISCUSSION

The measured surface doses of the thyroid and uterus and the dose at the scan center in both the PA spine and femur scan modes were smaller than the manufacturer's quoted values of 9.6 μGy (17). Also, these values are much lower than the average daily background in the United Kingdom of 7 μSv (18).

In this study, there was a significant correlation between the dose at the scan center and the thyroid and uterus surface doses ($p$-value < 0.01) (Fig. 5).

There was also a significant correlation between the thyroid and uterus surface doses ($p$-value < 0.05) (Fig. 6).

After regression analysis, the linear regression function between the thyroid surface dose ($D_s$ [thyroid]) and the uterus surface dose ($D_s$ [uterus]) was described by

$$D_s\,(thyroid) = D_s\,(uterus) \times 0.91 - 0.01$$

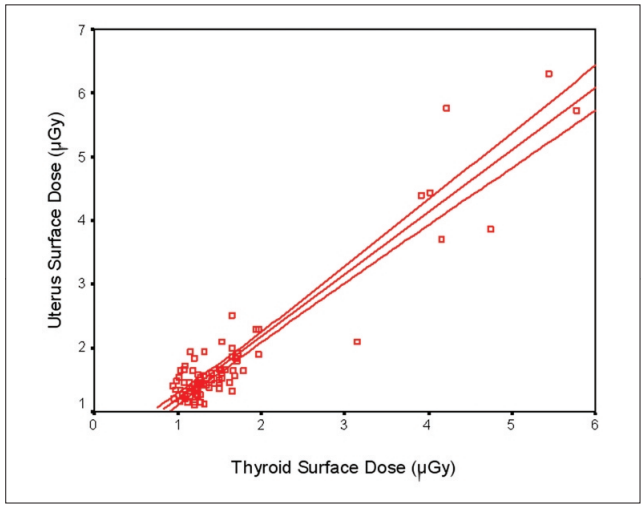


**Fig. 6.** Scatter plot between uterus surface dose and thyroid surface dose (μGy) with 95% confidence interval.

Based on the fact that the system has a pencil beam and the absorbed dose to the critical organs is due to scattered radiation, the significant correlation between the dose at the scan center and the organs' surface doses is remarkable. During the PA spine scan, for the phantom measurements, the absorbed doses to the uterus and the left and

right lobes of the thyroid were 1.21 ±0.33, 1.28 ±0.25 and 1.18 ±0.17 μGy, respectively. The average uterus surface dose in the femur scan was 2.52 ±1.12 μGy. Because the thyroid dose was on the same order of magnitude as the background, it was not considered in this protocol. The surface dose at the scan center was 7.38 ±2.27 μGy. All of these values are smaller than those the manufacturer reported for this scan mode (17). The contribution of the uterus, ovaries and the left and right thyroid on the effective dose in the PA spine scan was 0.06 ±0.02, 0.24 ± 0.07, 0.06 ±0.01 and 0.06 ±0.02 μSv, respectively. In the femur scan, the contributions of the uterus and ovaries to the effective dose were 0.13 ±0.06 and 0.50 ±0.22 μSv, respectively. We found a significant correlation between the surface and depth doses in the thyroid and uterus with the PA spinal scan. There was also a significant correlation between the uterus surface and depth doses in the femur scan.

In another study, the dosimetry of Hologic QDR-1000 systems having a pencil beam and the Hologic QDR-2000 systems having a fan beam was determined with results similar to those obtained in the present study (19). Njeh et al. (13) measured the thyroid and gonadal doses in the lunar DPX-L system and they showed that the contributions of the thyroid and gonadal doses to the effective dose were about zero; the dose at the scan center was 6 μGy. If we consider the TLD error in this energy range, our results are in the same range as those of this prior study.

Steel et al. (4) worked on lunar Expert-XL systems. Their reported contribution of the uterus to the effective dose was larger than the present study, which could be due to the differences in the output beam properties (fan beam: 143 kVp). For a Hologic QDR-2000 system, the contribution of the uterus and ovaries to the effective dose was larger than our results because this system uses a fan beam (16). Koo et al. (20) reported that the surface dose at the scan center for children is 3 μGy, which was smaller than the value obtained in the present study (6.5 μGy). The absorbed doses to a fetus phantom in the first trimester with a pencil beam scanning the femur and PA spine were 2.7 and 1.2 μGy, respectively. During the 2nd and 3rd trimesters, the absorbed doses were 2.7 and 4.9 μGy, respectively, for the PA spine scan and 1.4 and 1 μGy, respectively, for the femur scan (11).

One source of error in this study was variance in the photon density and TLD precision. We found a significant correlation between the thyroid and uterus surface doses and the scan center dose. We also estimated the depth dose from the surface dose. The percentage of the surface dose with respect to the dose at the scan center shows that the thyroid and uterus receive 33% and 35% of the dose to the scan center, respectively. The contribution of the effective dose equivalent from the DXA shows that the dose values of DXA are smaller than those of radiographic experiments (21).

After acquisition of dose values, correlations between the dose at the scan center and the surface dose at critical organs were assessed. The correlation between the surface dose and the scan center dose existed in the patient studies, but not in the phantom studies. Comparing the organ dose with the dose at the scan center in the phantom showed that there was no significant correlation between these two parameters. The fact that no relation existed between the critical organs' absorbed dose and the dose at the scan center could be due to the pencil beam in the system. Therefore, for the phantom measurements, we suggest using a larger sample to assess the correlation between the surface doses and scan center dose. Moreover these organs aren't in the scan direction; therefore, their absorbed dose was due to scattered radiation from other tissues.

Our results showed that exposure in bone densitometry with a lunar DPX-MD was low at the level of the daily background dose. Therefore, the use of this system in a periodic manner should be of a low risk. We were able to estimate the thyroid, uterus and ovarian absorbed doses by measuring the dose at the scan center and the associated organ surface doses.

## References


1. Blinov NN, Gubenko MB and Utkin PM. Development of osteodensitometric equipment. *Biomed Eng* 2002;36:36-40
2. Diez F. Guidelines for the diagnosis of osteoporosis by densitometric methods. *J Manipulative Physiol Ther* 2002;25:403-415
3. Boudousq V, Kotzki PO, Dinten JM, Barrau C, Robert-Coutant C, Thomas E, et al. Total dose incurred by patients and staff from BMD measurement using a new 2D digital bone densitometer. *Osteoporos Int* 2003;14:263-269
4. Steel SA, Baker AJ, Saunderson JR. An assessment of the radiation dose to patients and staff from a Lunar Expert-XL fan beam. *Physiol Meas* 1998;19:17-26
5. Eiken P, Barenholdt O, Jensen LB, Gram J, Nielson SP. Switching from DXA pencil beam to fan beam. I: studies in vitro at four centers. *Bone* 1994;15:667-670
6. Eiken P, Kolthoff N, Barenholdt O, Hermansen H, Nielson SP. Switching from DXA pencil beam to fan beam. II: studies in vivo. *Bone* 1994;15:671-676
7. Royal college of radiologist and national radiological protection board. *Patient dose reduction in diagnostic radiology* (documents of the NRPB). 1991;London: HMSO, 1:3
8. Popovic M, McNiell FE, Webber CE, Chettle DR. *The effect of lead in bone densitometry*. Nuclear Instruments and Methods in Physics Research Section B 2004;213:599-602
9. Culton N, Pocock N. Evaluation of three spine phantoms for DXA QC. *Bone* 2000;27:48S
10. Dequeker J, Pearson J, Reeve J, Henley M, Bright J, Felsenberg D, et al. Dual x-ray absorptiometry--cross-calibration and normative reference ranges for the spin: results of a European

Community Concerted Action. *Bone* 1995;17:247-254
11. Kalender WA, Felsenberg D, Genant HK, Fischer M, Dequeker J, Reeve J. The European Spine Phantom-a tool for standardization and quality control in spinal bone mineral measurements by DXA and QCT. *Eur J Radiol* 1995;20:83-92
12. Abrahamsen B, Gram J, Hansen TB, Beck-Nielsen H. Cross calibration of QDR-2000 and QDR-1000 dual energy X-ray densitometers for bone mineral and soft-tissue measurements. *Bone* 1995;16:385-390
13. Njeh CF, Samat SB, Nightingale A, McNeil EA, Boivin CM. Radiation dose and in vitro precision in paediatric bone mineral density measurement using dual X-ray absorptiometry. *Br J Radiol* 1997;70:719-727
14. Njeh CF, Apple K, Temperton DH, Boivin CM. Radiological assessment of a new bone densitometer-the Lunar EXPERT. *Br J Radiol* 1996;69:335-340
15. Blake GM, Patel R, Lewis MK, Batchelor S. New generation dual X-ray absorptiometry: a comparison of pencil beam and fan beam systems. *Br J Radiol* 1996;11:S157
16. Damilakis J, Perisinakis K, Vrahoriti H, Kontakis G, Varveris H, Gourtsoyiannis N. Embryo/fetus radiation dose and risk from dual X-ray absorptiometry examinations. *Osteoporos Int* 2002;13:716-722
17. Buroker KD. *DPX series operator's manual*, 1998:45-80
18. Hughes JS, Shaw KB, O'Riordan MC. *Radiation exposure of the UK population: 1988 review*. National Radiation Protection Board (Report NRPB-R227) 1989;London: HMSO 32-36
19. Boutros M. *Radiation dose assessment to patients and staff from the new LEXXOS bone dosimeter MSc thesis in Medical Engineering and Physics 2003*; King's collage London: 45-63
20. Koo WW, Walters J, Bush AJ. Technical considerations of dual-energy X-ray absorptiometry-based bone mineral measurements for pediatric studies. *J Bone Miner Res* 1995;10:1998-2004
21. Hart D, Jones DG, Wall BF. *Coefficient for estimating effective doses from paediatric x-ray examinations (NRPB-R279)*. 1996;London: HMSO 24-27